The 2010 IEEE/RSJ International Conference on
Intelligent Robots and Systems
October 18-22, 2010, Taipei, Taiwan

Kinetostatic Danger Field - a Novel Safety Assessment for Human-Robot Interaction

Bakir Lacevic and Paolo Rocco

Abstract— **This paper presents a novel method for evaluating the danger within the environment of a robot manipulator. It is based on the introduced concept of *kinetostatic danger field*, a quantity that captures the complete state of the robot - its configuration and velocity. The field itself is invariant with respect to objects around the robot and can be computed in any given point of the workspace using measurements from the proprioceptive sensors. Moreover, all the computation can be performed in closed form, yielding compact algebraic expressions that allow for real time applications. The danger field is not only a meaningful indicator about the risk in the vicinity of the robot, but can also be fed back within control skills that implement some well known safety strategies like collision avoidance and virtual impedance control, provided that some environment perception is available in order to determine the points where the field should be computed. Kinematic redundancy for simultaneous task performance and danger minimization can be exploited. The methodology described in the paper is supported with simulation results.**

I. Introduction

The question of safety in the human-robot coexistence/cooperation has become essentially important recently, because of the growing requests for people and robots to share the same workspace and/or task. A large attention is therefore given to this matter in the literature. Previous works treat the issue of safety from various aspects.

In the work of Ikuta et al. [1], the safety strategies were classified as pre-contact or post-contact strategies. Moreover, they discussed the minimization of the risk in interaction by means of mechanical design and by means of control. Although the main issue was safety in human-care robot control and design, they introduced the first systematic quantitative methods (danger index, safety index, etc.) in safety evaluation, concerning human robot interaction in general. Hirzinger et al. [2], used a lightweight robot, capable of operating a payload equal to its own weight. Reduction of the weights of the moving parts intuitively limits the injuries due to collisions and is one of the main factors in intrinsic safety. Zinn et al. [3], used empirical formulas developed by the automotive industry to correlate head acceleration to injury severity (head injury criteria) in order to evaluate the potential for serious injury due to impact. The work was mainly oriented towards new actuation concepts in the human-friendly robot design. They stressed out the importance of joint torque control approach and series elastic actuation. Heinzmann and Zelinsky [4] proposed a control scheme for robotic manipulators that restricts the torque commands of a position control algorithm to values that comply to predefined quantitative safety restrictions. For that purpose, they defined a quantity called impact potential as a maximum impact force that a moving mechanical system can create in a collision with a static obstacle. Bicchi et al. [5] presented the variable impedance approach as a mechanical/control co-design that allows the mechanical impedance parameters (stiffness, damping and inertia) to vary rapidly and continuously during the task execution. This approach guarantees low levels of injury risk while minimizing negative effects on control performance. By solving the so-called safe brachistochrone problem, the authors have shown that low stiffness is required at high speed and vice versa. In the successive publications of Kulic and Croft [6], [7], [8], several specific safety strategies were presented, as a components of an extensive methodology for safe planning and control in human-robot interaction. They addressed the important issue of estimating the human intent and affective state during the interaction. The information about the intent or the state of the human is used within a planning and control strategy to improve safety and intuitiveness of the interaction. Further, several danger indices have been formulated and used as an input to a real-time trajectory generation. A motion strategy consists in minimizing the danger index during the stable robot operation. The information about the human state, intent and the environment is acquired using the computer vision based system and the measurement of some physiological signals. Henrich and Kuhn [10] divide all safety aspects of the robot behavior into four groups (states) that easily fit into the formalism of state transition diagram. A similar mechanism is used by Guiochet et al. [11] to develop quite rigorous framework to facilitate the specification of safety rules used by an independent safety monitor. Kuhn et al. [12] use readings from the camera and a force/torque sensor to obtain the maximum allowable velocity of the robot based on the relative posture of the robot and the human. Finally, in [13] and [14] comprehensive overviews of safe human-robot interaction are presented.

This work describes a novel safety/danger evaluation for the objects in the robot environment. The main contribution is the introduction of a quantity, the kinetostatic danger field, that captures the complete state of the manipulator in terms of position and velocity. Besides providing merely a safety estimation, the danger field appears to be an immediately applicable instrument for the control that ensures safety. In addition, the danger field we propose can be expressed in closed form via algebraic expressions and thus it does not represent a bottleneck for real time computability.

The authors are with the Dipartimento di Elettronica e Informazione, Politecnico di Milano, 20133 Milan, Italy (e-mail: lacevic@elet.polimi.it; rocco@elet.polimi.it)

The remainder of the paper is organized as follows. In Section II we define the concepts of elementary and cumulative danger field, while Section III describes the computation of cumulative kinetostatic danger field of the robot manipulator. In Section IV, we discuss the possibilities for exploiting the danger field for control. A control strategy for redundant robots is presented in Section V. In Section VI we present simulation results, while concluding remarks and future work directions are given in Section VII.

II. Danger Field Definition

Let T be a point mass whose position and velocity are given by $\mathbf{r}_t = (x_t\ y_t\ z_t)^T$ and $\mathbf{v}_t = (v_{tx}\ v_{ty}\ v_{tz})^T$ respectively. For convenience, we set $\rho_t = \|\mathbf{r} - \mathbf{r}_t\|$ and $v_t = \|\mathbf{v}_t\|$, where $\mathbf{r} = (x\ y\ z)^T$ is a generic point in the world frame. Further, we define $\varphi = \angle(\mathbf{r} - \mathbf{r}_t, \mathbf{v}_t) \in [-\pi, \pi)$ as the angle between vectors $\mathbf{r} - \mathbf{r}_t$ and $\mathbf{v}_t$.

Definition 2.1: A differentiable scalar function $DF_R = DF_R(\mathbf{r}, \mathbf{r}_t)$ is called a static danger field if it satisfies the conditions:

i) $\exists f_R : \mathbb{R}^+ \to \mathbb{R}^+$, such that $DF_R(\mathbf{r}, \mathbf{r}_t) \equiv f_R(\rho_t)$,

ii) $\frac{df_R(\rho_t)}{d\rho_t} < 0,\ \forall \rho_t > 0$.

The static danger field (SDF) is obviously a radial scalar field, evaluated around the point $\mathbf{r}_t$ that represents the "source of danger". Consequently, isosurfaces of the field are concentrated spheres with the center in $\mathbf{r}_t$. The further away the point $\mathbf{r}$ gets from $\mathbf{r}_t$, the smaller the danger field $DF_R(\mathbf{r}, \mathbf{r}_t)$ becomes.

Definition 2.2: A differentiable scalar function $DF = DF(\mathbf{r}, \mathbf{r}_t, \mathbf{v}_t)$ is called a kinetostatic danger field if it satisfies the conditions:

i) $\exists f : \mathbb{R}^3 \to \mathbb{R}^+$, such that $DF(\mathbf{r}, \mathbf{r}_t, \mathbf{v}_t) \equiv f(\rho_t, v_t, \varphi)$,

ii) $DF(\mathbf{r}, \mathbf{r}_t, \mathbf{0})$ is a SDF,

iii) $\frac{\partial f(\rho_t, v_t, \varphi)}{\partial \rho_t} \equiv -\eta < 0,\ \forall \rho_t > 0,\ \forall v_t \geq 0,\ \forall \varphi \in [-\pi, \pi)$,

iv) $\frac{\partial f(\rho_t, v_t, \varphi)}{\partial v_t} > 0,\ \forall \rho_t > 0,\ \forall v_t \geq 0,\ \forall \varphi \in \left(-\frac{\pi}{2}, \frac{\pi}{2}\right)$,

v) $\varphi \frac{\partial f(\rho_t, v_t, \varphi)}{\partial \varphi} < 0,\ \forall \rho_t > 0,\ \forall v_t \geq 0,\ \forall \varphi \in [-\pi, \pi)$.

Beside the influence of the distance (condition *iii*)), the kinetostatic danger field (KSDF) captures two important aspects from the motion of the danger source. The first is the norm of the velocity vector (condition *iv*)), and the second is the declination angle φ between the velocity vector $\mathbf{v}_t$ and the vector $\mathbf{r} - \mathbf{r}_t$ that joins the danger source with the point where the danger field is computed. Since the motion direction of the source is taken into consideration, isosurfaces are no longer spheres (see Fig.1). This implies that the gradient of the KSDF is not necessarily collinear with the gradient of the corresponding SDF, i.e. the radial ray $\mathbf{r} - \mathbf{r}_t$. The following theorem provides an upper bound on the angle between these gradients. The proof is omitted for brevity.

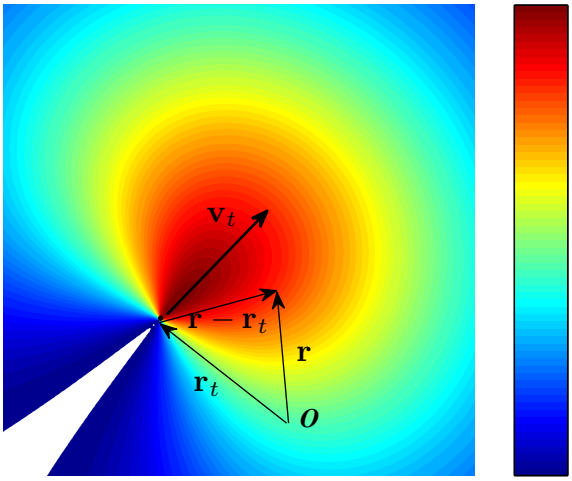

Fig. 1. Contours of the 2D KSDF example. O is the origin of the world frame.

Theorem 2.1: The angle δ between the gradients $\nabla DF(\mathbf{r}, \mathbf{r}_t, \mathbf{v}_t)$ and $\nabla DF(\mathbf{r}, \mathbf{r}_t, \mathbf{0})$ is such that:

$$\cos\delta = \left[1 + \eta^{-2}\rho_t^{-2}\left(\frac{\partial f}{\partial \varphi}\right)^2\right]^{-\frac{1}{2}} \tag{1}$$

where $\nabla = \left(\frac{\partial}{\partial x}\ \frac{\partial}{\partial y}\ \frac{\partial}{\partial z}\right)^T$ is the nabla operator.

Theorem 2.1 implies that nonzero $\frac{\partial f}{\partial \varphi}$ explicitly renders δ nonzero. On the other hand, the increase of ρ_t (moving away from the source) mitigates the contribution of motion within KSDF.

We now extend the principle of KSDF in the sense that the danger source is no longer a point, but a part of a curve moving in $\mathbb{R}^3$. Let $\mathbf{r}_t : [0, S] \to \mathbb{R}^3$ be the mapping that represents the piecewise smooth curve $\mathbf{r}_t(s) = (x(s)\ y(s)\ z(s))^T$, where s is the natural parameter and S is the length of the curve. Further, let $\mathbf{v}_t : [0, S] \to \mathbb{R}^3$ represent the mapping $\mathbf{v}_t(s) = (v_x(\mathbf{r}_t(s))\ v_y(\mathbf{r}_t(s))\ v_z(\mathbf{r}_t(s)))^T$ that assigns a certain velocity vector $\mathbf{v}_t(s)$ to each point of the curve $\mathbf{r}_t(s)$.

Definition 2.3: If $DF(\mathbf{r}, \mathbf{r}_t, \mathbf{v}_t)$ is KSDF, then the cumulative kinetostatic danger field *(*CKSDF*)* is defined as the following line integral:

$$CDF(\mathbf{r}) = \int_0^S DF(\mathbf{r}, \mathbf{r}_t, \mathbf{v}_t) ds \tag{2}$$

CKSDF captures the contribution of both position and motion of the curve in $\mathbb{R}^3$. Clearly, the concept of CKSDF can easily be extended to moving surfaces or bodies.

III. CKSDF of the Robotic Arm

A. Definitions

It is possible to define the CKSDF of the rigid robot manipulator using (2), where the curve over which the integration is performed is the line approximation of the kinematic chain. Knowing the position and the velocity of the link endpoints (obtainable from the proprioceptive sensors

measurements), one could evaluate both the position and velocity of any point on the chain just by using direct kinematics. Further, it is natural to compute the contribution of each link separately and then obtain the CKSDF as the superposition of these contributions. Let $\mathbf{r}_i$ and $\mathbf{r}_{i+1}$ be the positions of the endpoints of link i and let $\mathbf{v}_i$ and $\mathbf{v}_{i+1}$ be the corresponding linear velocities. Any point $\mathbf{r}_s$ on the link i could be represented as:

$$\mathbf{r}_s = \mathbf{r}_i + s\,(\mathbf{r}_{i+1} - \mathbf{r}_i)\,, \quad s \in [0,1] \tag{3}$$

Performing time derivation of (3), a similar property is obtained for the linear velocity of any point on the link i:

$$\mathbf{v}_s = \mathbf{v}_i + s\,(\mathbf{v}_{i+1} - \mathbf{v}_i)\,, \quad s \in [0,1] \tag{4}$$

Now, we can express some characteristic quantities that play role in the expressions for KSDF and CKSDF. First of all:

$$\mathbf{r} - \mathbf{r}_s = \begin{bmatrix} x \\ y \\ z \end{bmatrix} - \begin{bmatrix} r_{ix} + s(r_{i+1\,x} - r_{ix}) \\ r_{iy} + s(r_{i+1\,y} - r_{iy}) \\ r_{iz} + s(r_{i+1\,z} - r_{iz}) \end{bmatrix} \equiv \begin{bmatrix} \alpha_1 + \alpha_2 s \\ \beta_1 + \beta_2 s \\ \gamma_1 + \gamma_2 s \end{bmatrix}. \tag{5}$$

The module of the above vector is $\rho_s^2 = \|\mathbf{r} - \mathbf{r}_s\|^2 = as^2 + bs + c$, where $a = \alpha_2^2 + \beta_2^2 + \gamma_2^2$, $b = 2(\alpha_1\alpha_2 + \beta_1\beta_2 + \gamma_1\gamma_2)$ and $c = \alpha_1^2 + \beta_1^2 + \gamma_1^2$. The velocity vector is given with:

$$\mathbf{v}_s = \begin{bmatrix} v_{ix} + s(v_{i+1\,x} - v_{ix}) \\ v_{iy} + s(v_{i+1\,y} - v_{iy}) \\ v_{iz} + s(v_{i+1\,z} - v_{iz}) \end{bmatrix} \equiv \begin{bmatrix} a_1 + a_2 s \\ b_1 + b_2 s \\ c_1 + c_2 s \end{bmatrix}, \tag{6}$$

while its module is $v_s^2 = \|\mathbf{v}_s\|^2 = As^2 + Bs + C$, where $A = a_2^2 + b_2^2 + c2^2$, $B = 2(a_1a_2 + b_1b_2 + c_1c_2)$ and $C = a_1^2 + b_1^2 + c_1^2$. Further we need to determine the angle $\varphi = \angle(\mathbf{r} - \mathbf{r}_s, \mathbf{v}_s)$. Convenient approach would be to use the scalar product:

$$\cos\varphi = \frac{\langle \mathbf{r} - \mathbf{r}_s, \mathbf{v}_s \rangle}{\|\mathbf{r} - \mathbf{r}_s\|\|\mathbf{v}_s\|} = \frac{Ms^2 + Ns + P}{\sqrt{as^2 + bs + c}\sqrt{As^2 + Bs + C}}, \tag{7}$$

where $M = \alpha_2 a_2 + \beta_2 b_2 + \gamma_2 c_2$, $N = \alpha_1 a_2 + \alpha_2 a_1 + \beta_1 b_2 + \beta_2 b_1 + \gamma_1 c_2 + \gamma_2 c_1$ and $P = \alpha_1 a_1 + \beta_1 b_1 + \gamma_1 c_1$. The CKSDF of the link i is then given with:

$$CDF_i(\mathbf{r}) = \int_0^1 DF(\mathbf{r}, \mathbf{r}_s, \mathbf{v}_s)ds = \int_0^1 f(\rho_s, v_s, \varphi)ds, \tag{8}$$

where all the quantities can be easily computed. Consequently, the CKSDF of the n-DOF robot is:

$$CDF(\mathbf{r}) = \sum_{i=1}^{n} CDF_i(\mathbf{r}). \tag{9}$$

The field $CDF(\mathbf{r})$ is by definition a scalar field. Nevertheless, a vector field can easily be constructed upon it. The most natural way to do so is by using its gradient:

$$\vec{CDF}(\mathbf{r}) = CDF(\mathbf{r})\frac{\nabla CDF(\mathbf{r})}{\|\nabla CDF(\mathbf{r})\|}. \tag{10}$$

Thus, $\vec{CDF}(\mathbf{r})$ is a vector, anchored in $\mathbf{r}$, with the intensity $CDF(\mathbf{r})$, pointing in the direction defined by $\nabla CDF(\mathbf{r})$.

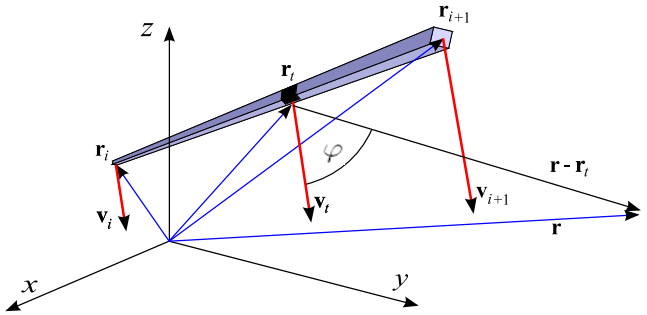

Fig. 2. Elements that play role in the computation of elementary danger field

B. An instance of the danger field

We propose the elementary KSDF, induced by the motion of infinitesimal portion of the link, as:

$$DF(\mathbf{r}, \mathbf{r}_t, \mathbf{v}_t) = \frac{k_1}{\|\mathbf{r} - \mathbf{r}_t\|} + \frac{k_2\|\mathbf{v}_t\|\,[\gamma + \cos\angle(\mathbf{r} - \mathbf{r}_t, \mathbf{v}_t)]}{\|\mathbf{r} - \mathbf{r}_t\|^2} \tag{11}$$

where k_1, k_2 and $\gamma \geq 1$ are positive constants, $\mathbf{r}$ is a point in space at which the field is being computed, and $\mathbf{r}_t$ and $\mathbf{v}_t$ are position and velocity of the moving element (see Fig. 2). The CDF induced by the motion of the complete link is:

$$\begin{aligned} CDF(\mathbf{r}, \mathbf{r}_i, \mathbf{v}_i, \mathbf{r}_{i+1}, \mathbf{v}_{i+1}) &= k_1 \textstyle\int_0^1 \frac{dt}{\sqrt{at^2+bt+c}} \\ +k_2\gamma \textstyle\int_0^1 \frac{\sqrt{At^2+Bt+C}}{at^2+bt+c}dt &+ k_2 \textstyle\int_0^1 \frac{Mt^2+Nt+P}{(at^2+bt+c)^{3/2}}dt, \end{aligned} \tag{12}$$

All integrals in (12) are solvable analytically and hence, the value of the danger field at any point of the space can be evaluated via an algebraic expression. Inputs to the expression are $\mathbf{r}_i, \mathbf{v}_i, \mathbf{r}_{i+1}, \mathbf{v}_{i+1}$ (all of them obtainable from direct kinematics) and a generic position $\mathbf{r}$. As previously stated, by simple superposition of the influences of arbitrarily many articulated links, one could obtain the danger field induced by the complete kinematic chain. Thus, the danger field of the complete robot is closed-form computable in an arbitrary position $\mathbf{r}$ using only the measurements from the proprioceptive sensors. However, in order to use the danger field for control purposes, we have to determine the positions $\mathbf{r}$ of relevant subjects/obstacles where the danger field needs to be computed. Clearly, this requires some kind of environment perception via exteroceptive sensors (e.g. cameras, lasers, etc.). For the primary representation of the concept we will assume that the problem of detecting the obstacles is solved and that the reasonably accurate estimation of the obstacles' locations is available. This is a common sense assumption since the solutions to the problem above are omnipresent in the robotic literature and practice (see e.g. [7], [12], [15]).

Fig. 3 shows the contour plot of the field induced by the motion of a 2DOF planar manipulator.

IV. Danger Field Based Control

Beside the pure danger measure of the subject(s) in the vicinity of the robot, the danger field represents usable information that could purposely shape the strategy of the

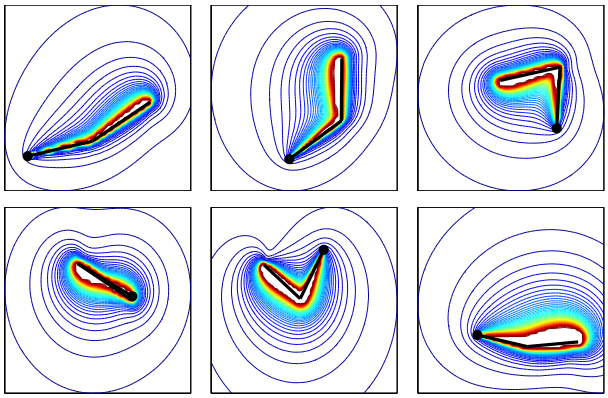

Fig. 3. Snapshots of the danger field's contour plot - a 2DOF example: both links accelerate in the counterclockwise direction (the robot base is marked)

robot control. Its role within the control system should ensure the decrease of the danger itself.

There is an obvious connection between the danger field and the ubiquitous potential field method used for the obstacle avoidance [15]. However, two big differences emerge. The first is that the source of the danger field is the robot itself, rather than the subject/obstacle. The second is that the classical potential field does not capture the velocity of the robot (nor the obstacle). On the other hand, the velocity certainly plays a significant part in danger assessment that could be observed as the estimation of the effects of the possible collision between the robot and the obstacle. For previous attempts to account for velocity in control and planning based on potential field (mostly for mobile platforms), the reader is referred to [16], [17], [18], [19].

As for the safety-oriented reactive control, our approach is considerably motivated by the extensive work of Kulic and Croft [7], where the control is shaped by a devotedly designed danger index. However, the real time algorithm therein relies on danger assessment that is based on a discrete number of points on the manipulator (critical points) and does not consider the kinematic chain as a whole. In addition, the issue of task consistency has not been tackled. Finally, their strategy is prevailingly descriptive and not easily reproducible since it depends on the other components of a broader framework (see e.g., [6]).

The method proposed in this paper also resembles the so called virtual (or visual) impedance approach [20], [21]. In this method, a virtual force is generated based on the penetration of the finite number of robot locations (usually just the end-effector) beyond a virtual surface surrounding an obstacle. The virtual force combines (in linear manner) the depth of the penetration, the corresponding velocity and the acceleration, thus emulating the classical impedance approach that considers a real physical contact between a robot and the environment. This force is then mapped to the joint torques via transposed Jacobian. The concept of virtual force will be extensively utilized within the danger field based control. The connection is quite intuitive: the vector of the danger field at the location of interest can be interpreted as the virtual force, or be the input argument to the virtual force - in a similar manner as the electrostatic force depends on the electrostatic field and the charge immersed in it. However, the difference between the two approaches are obvious. The danger field captures the kinematic behavior of the complete robot manipulator, while the virtual impedance control operates on a finite number of points on the robot. In addition, no virtual surfaces around the obstacles are considered in the danger field approach. We may refer to the family of isosurfaces of the danger field (see Fig. 3) as those virtual surfaces, with the distinction that they are "constructed" around the robot, not the obstacle. Finally, the danger field comprises the information about the posture and the velocity in a nonlinear way and hence can be treated as the generalized non-linear virtual impedance. Its intuitive definition, that is an attempt to establish a comprehensive, yet simple danger/safety assessment makes it a good ingredient for the design of the control system that ensures safe human-robot interaction.

V. Control of Multi DOF Robots

The danger field proposed in this paper can be used in the control of a multi DOF robot. The dynamic equations of the robot in the joint space are:

$$\mathbf{M}(\mathbf{q})\ddot{\mathbf{q}} + \mathbf{b}(\mathbf{q},\dot{\mathbf{q}}) + \mathbf{g}(\mathbf{q}) = \mathbf{T}, \tag{13}$$

where $\mathbf{q} \in \mathbb{R}^n$ is the vector of n joint coordinates, $\mathbf{M}(\mathbf{q}) \in \mathbb{R}^{n\times n}$ is the symmetric non-singular inertia matrix, $\mathbf{b}(\mathbf{q},\dot{\mathbf{q}}) \in \mathbb{R}^n$ is the vector of torques due to centripetal, Coriolis and friction forces, $\mathbf{g}(\mathbf{q}) \in \mathbb{R}^n$ is the vector of torques due to gravity and $\mathbf{T} \in \mathbb{R}^n$ is the vector of joint torques.

Assume that the task space has m dimensions. The corresponding task space model is given by [22]:

$$\mathbf{A}(\mathbf{q})\ddot{\mathbf{x}} + \mathbf{h}(\mathbf{q},\dot{\mathbf{q}}) + \mathbf{p}(\mathbf{q}) = \mathbf{F}, \tag{14}$$

where $\mathbf{A}(\mathbf{q}) = \left(\mathbf{J}(\mathbf{q})\mathbf{M}^{-1}(\mathbf{q})\mathbf{J}^T(\mathbf{q})\right)^{-1} \in \mathbb{R}^{m\times m}$, with $\mathbf{J}(\mathbf{q}) \in \mathbb{R}^{m\times n}$ being a Jacobian. $\mathbf{F} \in \mathbb{R}^m$ represents the force in the operational space. Vectors $\mathbf{h}(\mathbf{q},\dot{\mathbf{q}}) \in \mathbb{R}^m$ and $\mathbf{p}(\mathbf{q}) \in \mathbb{R}^m$ are given by:

$$\mathbf{h}(\mathbf{q},\dot{\mathbf{q}}) = \bar{\mathbf{J}}^T(\mathbf{q})\mathbf{b}(\mathbf{q},\dot{\mathbf{q}}) - \mathbf{A}(\mathbf{q})\dot{\mathbf{J}}(\mathbf{q})\dot{\mathbf{q}}, \tag{15}$$

$$\mathbf{p}(\mathbf{q}) = \bar{\mathbf{J}}^T(\mathbf{q})\mathbf{g}(\mathbf{q}), \tag{16}$$

where $\bar{\mathbf{J}}(\mathbf{q}) = \mathbf{M}^{-1}(\mathbf{q})\mathbf{J}^T(\mathbf{q})\mathbf{A}(\mathbf{q})$ is the dynamically consistent generalized inverse [22].

Assume there are $N \in \mathbb{N}$ relevant obstacles in the robot environment and let $\mathbf{r}_j$ be the position of the obstacle j, $j \in \{1,2,\ldots,N\}$. We may refer to $\mathbf{r}_j$ as to position of the point on the obstacle that is the nearest to the robot. Define m as:

$$m = \begin{cases} 1 & \text{if } \|\vec{CDF}(\mathbf{r}_j)\| \le \Delta_j,\ \forall j \in \{1,2,\ldots,N\} \\ 0 & \text{otherwise,} \end{cases} \tag{17}$$

meaning that $m = 1$ if and only if the value of the danger field at each of the relevant locations $\mathbf{r}_j$ does not exceed a certain threshold Δ_j. Inspired by the frameworks described in [9] and [21] we propose the control law:

$$\mathbf{T} = m\mathbf{T}_{task} + [(1-m)\mathbf{I} + m\mathbf{N}^T(\mathbf{q})]\mathbf{T}_{subtask}. \tag{18}$$

The torque $\mathbf{T}_{task}$ is responsible for the task behavior. If $m=1$, then the subtask torque $\mathbf{T}_{subtask}$ affects only the robot posture, without altering the end effector dynamic behavior. This is guaranteed by the matrix $\mathbf{N}(\mathbf{q}) = \mathbf{I} - \bar{\mathbf{J}}(\mathbf{q})\mathbf{J}(\mathbf{q})$ that projects an arbitrary torque vector into the null-space of $\bar{\mathbf{J}}^T(\mathbf{q})$. If $m=0$, $\mathbf{T}_{subtask}$ affects the dynamics of the complete robot. We construct the torque $\mathbf{T}_{subtask}$ as:

$$\mathbf{T}_{subtask} = \sum_{j=1}^{N} \sum_{k=1}^{n} \mathbf{J}^T(\mathbf{q}, j, k) \mathbf{F}_k \left(\vec{CDF}(\mathbf{r}_j), \dot{\mathbf{r}}_j \right), \qquad (19)$$

where $\mathbf{J}(\mathbf{q}, j, k)$ is a Jacobian matrix associated with the point on the link k that is the closest to the subject/obstacle j.

Vector functions $\mathbf{F}_k : \mathbb{R}^6 \to \mathbb{R}^3$, $k \in \{1, 2, \ldots, n\}$, represent the virtual forces that are (in general) dependent on the danger field vector $\vec{CDF}(\mathbf{r}_j)$ at the position $\mathbf{r}_j$ and the subject/obstacle velocity $\mathbf{v}_j$. Intuitively, the force $\mathbf{F}_k$ should increase with the decrease of the angle between $\mathbf{v}_j$ and $\vec{CDF}(\mathbf{r}_j)$. The obvious drawback of this approach is the necessity to estimate the obstacle's velocity. Thus, from now on, we assume that the force $\mathbf{F}_k = k_F \vec{CDF}(\mathbf{r}_j)$, where k_F is a positive parameter.

The above choice of the subtask behavior leads to decrease of the overall danger while performing the specified task ($m=1$). If the danger exceeds certain limit, the task behavior becomes relaxed ($m=0$) and control leads to the decrease of the danger without the task consistency. If necessary, the signal m may be processed by a low-pass filter before applying it within (18) in order to obtain a smooth transition. The above control strategy is designed prevailingly for redundant manipulators. For non-redundant case, the matrix $\bar{\mathbf{J}}(\mathbf{q})$ is equal to $\mathbf{J}^{-1}$ and $\mathbf{N}$ becomes a zero matrix. Consequently, $\mathbf{T}_{subtask}$ can affect the motion of the robot only if $m=0$.

Although primarily intended to ensure a collision-free behavior, the danger field based control can easily be modified to scenarios that require the physical contact between the robot and a human operator. Assume that the end-effector trajectory that assures the intended contact cooperation (e.g. placing an object in a human's hand whose location is $\mathbf{r}_p$) is enabled via control input $\mathbf{T}_{task}$. By setting the threshold Δ_p large enough, the proximity between the hand and the end effector will not cause the task suspension and the assignment can successfully be completed.

Note that the control approach described in this section is not designed a priori to achieve a fail-safe performance. Nevertheless the proposed control scheme can be embedded into a larger scope framework, whose architecture would contain an independent fail-safe monitoring system.

VI. Simulation Results

For the simulation purposes, we use a dynamic model of a 6 DOF robot with revolute joints. The robot is modeled using the Robotics Toolbox for Matlab [23]. The first simulation scenario considers the subject/obstacle avoidance while the task is to keep the end-effector where it is. The spherical obstacle moves along a straight line (see Fig.4) in the way that the minimum distance between the robot and the obstacle slightly decreases. The danger field at the obstacle's location

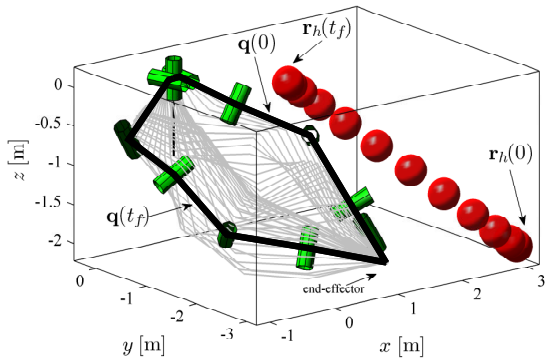

Fig. 4. Null-space motion with subject/obstacle avoidance

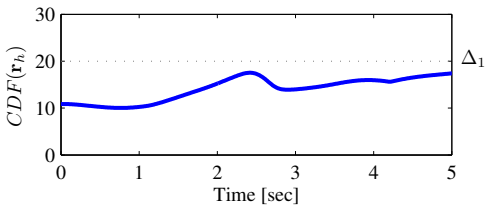

Fig. 5. Profile of the cumulative danger field

(the point on the obstacle that is the closest to the robot) does not exceed the threshold (the value $\Delta_1 = 20$ is assumed) (Fig.5), which implies the consistency of the task, i.e. the robot performs the null-space motion while its kinematic redundancy is exploited for reaching less dangerous postures. The initial and the final posture of the robot ($\mathbf{q}(0)$ and $\mathbf{q}(t_f)$ respectively) as well as the initial and the final position of the obstacle ($\mathbf{r}_h(0)$ and $\mathbf{r}_h(t_f)$ respectively) are indicated. We set the simulation time $t_f = 5$sec.

In the second scenario, the obstacle moves along a circumference and gets very close to the end-effector at one point. This induces the necessity for the suspension of the task (keeping the end-effector still), because the danger field at the obstacle's location exceeds the threshold Δ_1. Consequently, the end effector leaves the target position while the danger field at the subject location remains nearly constant. The task resumption will follow shortly after the value of the danger field drops below the given threshold (see Figs 6 and 7).

VII. Conclusions and Future Works

This paper presented a novel method for estimating the danger level in the vicinity of a robot manipulator. The method stands upon the introduced concept of kinetostatic danger field that is the generalization of well known potential field approach. Two main differences are that the danger field captures both the posture and the velocity of the robot and that the source of the field is the robot itself, rather than the subject/obstacle. Besides the comprehensive information about the danger level, the danger field appears to be the useful control tool that increases the degree of safety in the interaction. Another benefit of the method described

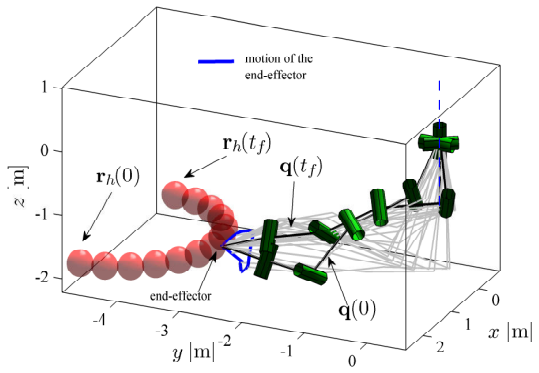

Fig. 6. Exceeding the danger field threshold induces task suspension

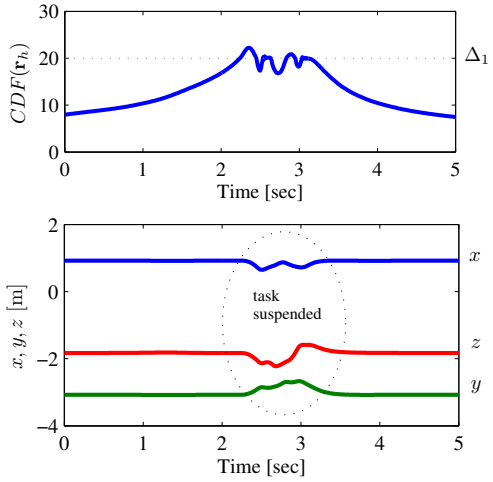

Fig. 7. The profile of the cumulative danger field and the profiles of the end-effector's coordinates

is the closed form computability that allows for the real time applications. The method presented was subjected to simulations for multi DOF robot.

Further research will include the experimental validation of the described concept using a multi DOF robot. Moreover, the motion planning with the embedded safety heuristic will be investigated in order to make further steps towards a unified safety oriented framework.

VIII. Acknowledgments

The research leading to these results has received funding from the European Community's Seventh Framework Programme FP7/2007-2013 - Challenge 2 - Cognitive Systems, Interaction, Robotics - under grant agreement No 230902 - ROSETTA.

References

[1] K. Ikuta, M.Nokata, H.Ishii, Safety Evaluation Method of Design and Control for Human-Care Robots, *The International Journal of Robotics Research*, 2003, Vol. 22, No. 5, pp 281-297

[2] G. Hirzinger, A. Albu-Schffer, M. Hhnle, I. Schaefer, N. Sporer, A new generation of torque controlled light-weight robots, *Proc. Int. Conf. Robotics Automation*, 2001, Seoul, Korea, pp 3356-3363.

[3] M. Zinn, O. Khatib, B. Roth, J.K. Salisbury, Playing it safe (human-friendly robots), *Robotics and Automation Magazine*, June 2004, IEEE Volume 11, Issue 2, pp 12-21

[4] J. Heinzmann and A. Zelinsky, Quantitative safety guarantees for physical human-robot interaction, *The International Journal of Robotics Research*, 2003, vol. 22, no. 7/8, pp. 479-504

[5] A. Bicchi, G. Tonietti, Fast and Soft Arm Tactics - Dealing with the Safety-Performance Trade-Off in Robot Arms Design and Control, *IEEE Robotics and Automation Magazine, Special issue on Dependability in Human-Friendly Robots*, June 2004, Vol. 11, No. 2

[6] D. Kulic, E. Croft, Safe Planning for Human-Robot Interaction, *Journal of Robotic Systems* 2005, Vol. 22, No. 7, pp 383 - 396

[7] D. Kulic, E. Croft, Real-time safety for human-robot interaction, *Robotics and Autonomous Systems*,Jan 31, 2006, v54, n1, pp 1-12

[8] D. Kulic, E. Croft, Affective State Estimation for Human-Robot Interaction, *IEEE Transactions on Robotics*, Vol. 23, No. 5, pp. 991 - 1000, 2007

[9] O. Brock, O. Khatib, Elastic Strips: A Framework for Motion Generation in Human Environments *International Journal of Robotics Research*, Vol. 21, No. 12, Dec 2002, pp. 1031-1052

[10] D. Henrich, S. Kuhn, Modeling Intuitive behavior for safe human/robot coexistence cooperation, *Robotics and Automation, Proceedings 2006 IEEE International Conference on*, vol., no., pp.3929-3934, 15-19 May 2006

[11] J. Guiochet, D. Powell, E. Baudin, J.-P. Blanquart, Online safety monitoring using safety modes, *6th IARP/IEEE-RAS/EURON Workshop on Technical Challenges for Dependable Robots in Human Environments*, Pasadena, CA, USA (May 2008)

[12] S. Kuhn, T. Gecks, D. Henrich, Velocity Control for Safe Robot Guidance Based on Fused Vision and Force/torque Data, *Proc. IEEE Conference on Multisensor Fusion and Integration*, 3-6 September, 2006, Heidelberg, Germany

[13] R. Alami, A. Albu-Schaeffer, A. Bicchi, R. Bischoff, R. Chatila, A. De Luca, A. De Santis, G. Giralt, J. Guiochet, G. Hirzinger, F. Ingrand, V. Lippiello, R. Mattone, D. Powell, S. Sen, B. Siciliano, G. Tonietti, and L. Villani, Safe and Dependable Physical Human-Robot Interaction in Anthropic Domains: State of the Art and Challenges, *Proc. IROS'06 Workshop on pHRI - Physical Human-Robot Interaction in Anthropic Domains*, 2006. IEEE

[14] A. Pervez, J. Ryu, Safe physical human robot interaction-past, present and future *Journal of Mechanical Science and Technology*, Vol. 22, No. 3. (5 March 2008), pp. 469-483.

[15] O. Khatib, O, Real-time obstacle avoidance for manipulators and mobile robots, *International Journal of Robotics Research*, 1986, 5(1), pp 9098.

[16] M. Khatib, R. Chatila, An extended potential field approach for mobile robot sensor-based motions, *Proc. of the Intelligent Autonomous Systems, IAS-4*, IOS Press, pp. 490496, 1995.

[17] R.B. Tilove, Local obstacle avoidance for mobile robots based on the method of artificial potentials, *Proc. IEEE Int. Conf. on Robotics and Automation*, pp.566-571, 13-18 May 1990.

[18] B.H. Krogh, A Generalized Potential Field Approach to Obstacle Avoidance Control, *Proceedings of the International Robotics Research Conference*, pp. 11501156, 1984.

[19] P. Fiorini, Z. Shiller, Motion planning in dynamic environments using the relative velocity paradigm, *Proc. IEEE Int. Conf. on Robotics and Automation*, pp.560-565, vol.1, 2-6 May 1993

[20] Y. Nakabo, M. Ishikawa, Visual impedance using 1 ms visual feedback system, *Proc. IEEE Int. Conf. on Robotics and Automation*, 16-20 May 1998, vol.3, no., pp 2333-2338.

[21] T. Tsuji, H. Akamatsu, M. Kaneko, Non-contact impedance control for redundant manipulators using visual information, *Proc. 1997 IEEE International Conference on Robotics and Automation* vol.3, pp.2571-2576, 20-25 Apr 1997.

[22] O. Khatib, Inertial properties in robotics manipulation: An object-level framework, *International Journal of Robotics Research*, 1995 14(1), pp 1936.

[23] P.I. Corke, A Robotics Toolbox for Matlab, *IEEE Robotics and Automation Magazine*, 1996, Vol. 3, No 1, pp 24-32.